Available online at www.sciencedirect.com
ScienceDirect
Agricultural and Forest Meteorology 140 (2006) 269–286
AGRICULTURAL AND FOREST METEOROLOGY
www.elsevier.com/locate/agrformet

Photosynthetic light use efficiency of three biomes across an east–west continental-scale transect in Canada

Christopher R. Schwalm [a,*], T. Andrew Black [a], Brian D. Amiro [b], M. Altaf Arain [c], Alan G. Barr [d], Charles P.-A. Bourque [e], Allison L. Dunn [f], Larry B. Flanagan [g], Marc-André Giasson [h], Peter M. Lafleur [i], Hank A. Margolis [h], J. Harry McCaughey [j], Alberto L. Orchansky [k], Steve C. Wofsy [f]

[a] *Faculty of Land and Food Systems, University of British Columbia, Vancouver, British Columbia V6T 1Z4, Canada*
[b] *Department of Soil Science, University of Manitoba, Winnipeg, Manitoba R3T 2N2, Canada*
[c] *School of Geography and Earth Sciences, McMaster University, Hamilton, Ontario L8S 4K1, Canada*
[d] *Climate Research Branch, Meteorological Service of Canada, Saskatoon, Saskatchewan S7N 3H5, Canada*
[e] *Faculty of Forestry and Environmental Management, University of New Brunswick, Fredericton, New Brunswick E3B 6C2, Canada*
[f] *Department of Earth and Planetary Science, Harvard University, Cambridge, MA 02138, USA*
[g] *Department of Biological Sciences, University of Lethbridge, Lethbridge, Alberta T1K 3M4, Canada*
[h] *Faculté de Foresterie et de Géomatique, Université Laval, Québec G1K 7P4, Canada*
[i] *Department of Geography, Trent University, Peterborough, Ontario K9J 7B8, Canada*
[j] *Department of Geography, Queen's University, Kingston, Ontario K7L 3N6, Canada*
[k] *Canadian Forest Service, Northern Forestry Centre, Edmonton, Alberta T6H 3S5, Canada*

Received 8 December 2005; accepted 27 June 2006

Abstract

Light use efficiency (LUE) is used widely in scaling and modeling contexts. However, the variation and biophysical controls on LUE remain poorly documented. Networks of eddy covariance (EC) towers offer an opportunity to quantify ε_g, the ratio of P, gross primary productivity, to Q_a, absorbed photosynthetically active radiation (PAR), across climate zones and vegetation types. Using data from the Fluxnet Canada Research Network ($n = 24$ sites) in 2004, we examined the relationship between daily and yearly ε_g, driving variables, and site characteristics on a site-specific and plant functional type (PFT) basis using tree regression and linear regression. Data were available for three biomes: grassland, forest, and wetland. Yearly ε_g values ranged from 0.1 to 3.6 g C MJ^{-1} Q_a overall. Daily ε_g was highest in the grassland (daily median ± interquartile range: 3.68 ± 1.98 g C MJ^{-1} Q_a), intermediate in the forested biome (0.84 ± 0.82 g C MJ^{-1} Q_a), and lowest for the wetlands (0.65 ± 0.54 g C MJ^{-1} Q_a). The most important biophysical controls were light and temperature, to the exclusion of water-related variables: a homogeneity of slopes model explained c. 75% of the variation in daily ε_g. For a subset of sites with diffuse PAR data, the ratio of diffuse to total PAR, a proxy for cloudiness, was a key predictor. On the yearly time scale, ε_g was related to leaf area index and mean annual temperature. Aggregating to PFTs did not show functional convergence within any PFT except for the three wetland sites and the *Picea mariana* toposequence at the daily time step, and when using the Köppen climate classification on a yearly time step. The general lack of conservative daily ε_g behavior within PFTs suggests that PFT-based parameterizations are inappropriate, especially when applied on shorter temporal scales.

Keywords: Photosynthetic light use efficiency; Eddy covariance; Carbon balance; Scaling; Functional convergence; Fluxnet Canada Research Network

* Corresponding author. Tel.: +1 604 822 9119; fax: +1 604 822 4400.
E-mail address: christopher.schwalm@ubc.ca (C.R. Schwalm).

0168-1923/$ – see front matter
doi:10.1016/j.agrformet.2006.06.010

1. Introduction

Light use efficiency (LUE) was first articulated in the context of agricultural systems (Monteith, 1972, 1977). Monteith's early work focused on the linear relationship between yield and solar irradiance. This concept has been extended into forested ecosystems and is currently used in several modeling platforms, most notably production efficiency models (e.g., Cramer et al., 1999a,b; Ruimy et al., 1999). Furthermore, the LUE concept is routinely used in deriving satellite-based estimates of primary production (Running et al., 2004) and serves as a scaling metric in global carbon (C) cycling studies (Nichol et al., 2000; Still et al., 2004; Turner et al., 2003b). Despite its widespread use variation in LUE and its biophysical controls remain poorly understood (Goetz and Prince, 1999; Green et al., 2003; Lagergren et al., 2005; Turner et al., 2003b), supporting critical assessment of LUE for production models, remote-sensing applications, and through direct field-based measurements (Norby et al., 2003).

An important issue is the lack of a universally agreed upon definition of LUE, a quotient where the numerator quantifies production and the denominator irradiance. Historically, the numerator has been defined as net primary productivity (NPP, aboveground or total) or gross primary productivity (P) while incident, intercepted, absorbed total shortwave or PAR have been used as denominators (Goetz and Prince, 1999; Gower et al., 1999). Methodological issues further confound uncertainty regarding the behavior of LUE. For example, direct measurements of NPP, especially the belowground component, are prone to large error (Gower et al., 1999). The net result is difficulty in comparing LUE estimates from disparate studies to elucidate the response of LUE to various environmental drivers relative to gradients in vegetation.

The proliferation of eddy covariance (EC) research installations holds promise in overcoming some of these difficulties. There are currently over 360 EC towers worldwide (http://www.fluxnet.ornl.gov/fluxnet/viewstatus.cfm). Most EC installations produce dense streams of data. In addition to flux measurements, meteorological, soil, and ecological data are also generally available. As P can be resolved from flux measurements through flux-partitioning and gap filling algorithms, a network of EC towers offer an opportunity to quantify LUE as well as its biophysical controls at various points around the globe using a unified methodology (e.g., Nichol et al., 2002; Turner et al., 2003b).

In addition to the importance of elucidating relationships between LUE and its biophysical controls there is a great need to determine if and how LUE varies by functional group (Gower et al., 1999). This is tied to functional convergence; the notion that a statistical population of LUE values can be partitioned into groups where LUE is conservative. These partitions or strata are usually defined as plant functional types (PFTs) based on some covariate, e.g., climate, site productivity, and vegetation type (Cramer, 1997). Initially, Monteith (1972) speculated that LUE would be invariant across species. Field (1991) and Goetz and Prince (1999) provided evolutionary and physiological arguments for convergence of LUE, based on NPP and P, respectively, within PFTs. Nonetheless, convergence, particularly with regards to NPP, has been elusive (Chen and Coughenour, 2004; Goetz and Prince, 1999; Gower et al., 1999; Ruimy et al., 1994; Runyon et al., 1994). Despite this, production efficiency models make use of PFT-specific LUE values, at times modified by reduction factors based on meteorological drivers. In addition to convergence considerations, the difference between remotely sensed and field-based estimates of productivity has been linked to estimates of LUE (Aalto et al., 2004; Ahl et al., 2004), supporting the use of EC-derived values to validate satellite-based estimates in the context of scaling (Turner et al., 2003a, 2005).

The objective of this study is to examine the behavior of LUE, daily, seasonal, and yearly, across the Fluxnet Canada Research Network (FCRN). In 2004, the FCRN was comprised of 29 EC sites laid out along an east–west continental-scale transect in the southern portion of Canada. Emphasis will be placed on how LUE varies in relation to biophysical controls and vegetation gradients. Given the range of sites and wealth of data, functional convergence between sites and model-based summaries will figure prominently. In addition, the effect of varying assumptions in the calculation of LUE is discussed.

2. Material and methods

2.1. Site characteristics

Data from a particular EC site was included in the study if a quality-controlled data record for 2004 was available. At a minimum a site needed to have meteorological and flux data as well as leaf area index (LAI). Of the 29 EC sites within the FCRN in 2004, including associated sites, 24 fulfilled these criteria (Table 1). These sites spanned three biomes (grassland, wetland, and forest) with most sites being situated in forested terrain. At all sites, the EC method was used to

Table 1
Summary of site characteristics

Site[a]	Vegetation type	Overstory	Understory and groundcover	LAI[b] ($m^2\ m^{-2}$)	Age (years)	Mean DBH (cm)	Canopy height (m)	Location (°)	Elevation (m)
DF49	Coniferous temperate rainforest	*P. menziesii*	*Achlys triphylla*, *Berberis aquifolium*, bryophytes	6.1 Ds	55	28.3	29.7	48.87N, 125.35W	320
EOBS	Coniferous boreal forest	*P. mariana*, *P. banksiana*	*Ericaceae*, bryophytes	4.0 Ds	c. 105	14.8	14	49.69N, 74.43W	387
EPL	Ombrotrophic bog; wetland	–	*Rhododendron groenlandicum*, *Chamaedaphne calyculata*, *Kalmia augustifoliam*, *Vaccinium myrtilloides*, bryophytes	1.3 Lp	–	–	Shrub: 0.25	45.41N, 75.52W	70
F77	Coniferous boreal forest	*P. banksiana*, *P. mariana*	*V. myrtilloides*	2.9 Ds	27	7	7.4	54.48N, 105.82W	590
F89	Coniferous boreal forest	*P. banksiana*, *Populus tremuloides*	*Alnus crispa*, *Rosa acicularis*	1.8 Ds	15	7	5	54.25N, 105.88W	536
F98	Coniferous boreal forest	*Dead P. banksiana*, *P. mariana*	*P. banksiana*, *P. mariana, P. tremuloides, Epilobium angustifolium*	1.0 Sp	6	Standing dead: 17	Standing dead: 20; live: 1	53.92N, 106.08W	540
FEN	Minerotrophic, patterned fen; wetland	–	*Larix laricina*, *Carex* spp.	1.0 Gp	–	–	–	53.78N, 104.62W	488
GRS	Short/mixed grass prairie (C3); grassland	–	*Agropyron dasystachyum*, *A. smithii*	0.7 **Be**	–	–	0.185	49.43N, 112.56W	951
HBS00	Coniferous boreal forest	–	*P. mariana*, *Kalmia* spp., *Vaccinium* spp., *R. groenlandicum*, bryophytes	0.8 Sp	4	–	–	49.27N, 74.04W	400
HDF00	Coniferous temperate rainforest	–	*P. menziesii*, *A. triphylla*, *B. aquifolium*, bryophytes, pteridophytes	2.2 **Pp**	4	1 (at base)	0.6	49.87N, 125.29W	180
HDF88	Coniferous temperate rainforest	*P. menziesii*	*Gaultheria shallon*, *B. aquifolium*, pteridophytes	4.4 **Ps**	16	7.3	5.8	49.52N, 124.90W	120
HJP02	Coniferous boreal forest	–	*P. banksiana*	1.3 **Mp**	2	–	0.1	53.95N, 104.65W	579
HJP75	Coniferous boreal forest	*P. banksiana*	*A. crispa*, lichens	4.3 Ds	29	–	–	53.88N, 104.65W	579
NOBS	Coniferous boreal forest	*P. mariana*	Bryophytes	4.1 Ls	c. 160	8.5	9.1	55.89N, 98.48W	259
OA	Deciduous boreal forest	*P. tremuloides*	*Corylus avellana*	3.8 **Ls**	86	21	21	53.63N, 106.20W	601
OBF	Coniferous maritime forest	*Abies balsamea*	*Cornus canadensis*, bryophytes, pteridophytes	6.1 **Ms**	35	12.9	13.5	46.47N, 67.10W	340
OJP	Coniferous boreal forest	*P. banksiana*	*A. crispa*, lichens	3.4 Ds	75	12.9	13.7	53.92N, 104.69W	579
OMW	Mixedwood temperate forest	*P. tremuloides*, *P. mariana*, *Picea glauca*, *Betula papyrifera*	*C. canadensis*, bryophytes, pteridophytes	4.1 Ds	c. 60	16.1	13.7	48.22N, 82.16W	341
SOBS	Coniferous boreal forest	*P. mariana*	Bryophytes	5.6 Ds	c. 125	7.1	13.7	53.99N, 105.12W	629

Table 1 (*Continued*)

Site[a]	Vegetation type	Overstory	Understory and groundcover	LAI[b] (m^2 m^{-2})	Age (years)	Mean DBH (cm)	Canopy height (m)	Location (°)	Elevation (m)
WPL	Treed fen; wetland	*L. laricina*, *P. mariana*	*Betula pumila*, *R. groenlandicum*, *Salix* spp., bryophytes	2.7 **Np**	*L. laricina*: 35 y *P. mariana*: 135 y	Trees: 2.9	Trees: 3	54.95N, 112.46W	626
WPP02	Coniferous temperate forest	–	*P. strobus*, various forbs, herbaceous plants	0.8 Pp	2	1.5	0.9	42.66N, 80.56W	265
WPP39	Coniferous temperate forest	*P. strobus*	*Prunus serotina*, *Quercus alba*, *Q. velutina*, *A. balsamea*, *Rhus radicans*, pteridophytes, bryophytes	3.5 Ps	65	34.6	22	42.71N, 80.36W	184
WPP74	Coniferous temperate forest	*P. strobus*	Bryophytes	3.5 Ps	30	15.6	12	42.71N, 80.35W	184
WPP89	Coniferous temperate forest	*P. strobus*	–	6.5 Ps	15	15.8	9	42.78N, 80.46W	212

Vegetation characteristics were surveyed between 2001 and 2005; age references 2004. Dashed entries indicate no data available or missing data.

[a] Site names are composed of codes containing information about location, establishment year, and site history. The last two numbers indicate when the stand was established, e.g., 74 = 1974. Multi-cohort stands generally lack these trailing digits. The following characters have specific meanings: E, eastern, located in Quebec; F, the site was burned; H, the stand was harvested; N, located in former BOREAS northern study area in Manitoba; O, old, stand age >70 except for OBF; S, located in former BOREAS southern study area in Saskatchewan; W, western, located in Alberta. Other letter combinations reference the common name of the dominant vegetation: A, aspen; BF, balsam fir; BS, black spruce; DF, Douglas-fir; JP, jack pine; PL, peatland; WPP, white pine plantation (other stands have natural regeneration and occasionally some planted stock).

[b] Capitalized character indicates source of LAI (values in bold have seasonal trajectory, daily maximum is shown): B, interpolation using periodic biomass measurements and peak LAI; D, digital hemispherical photography; G, guesstimate, the mid-point of the BOREAS LAI data were used; L, published report: Moore et al. (2002) for EPL, Turner et al. (2003b) for NOBS, and Barr et al. (2004) for OA; M, MODIS subset, only the pixel containing the tower; N, interpolation using periodic tower-based estimated NDVI and peak LAI; P, LAI-2000 (LI-COR, Lincoln, NE, USA), either one value per year or interpolated to daily values; S, destructive sampling; summer 2003 for F98, summer 2005 for HBS00. Lower-case character indicates leaf angle distribution assumed in Q_a calculations: e, erectophile; p, planophile; s, spherical.

measure CO_2 fluxes to obtain net ecosystem productivity (F_{NEP}). Fluxes were corrected for storage in the air column, block-averaged every 30 min, and missing values from low turbulence or instrumentation failure were gap filled. Positive F_{NEP} indicated sequestration of CO_2; P and ecosystem respiration (R) were always positive. Only 17 sites had continuous year round EC data coverage with the remainder having either only the growing season (c. June–September) or sporadic coverage, i.e., a roving EC system shared among multiple sites (Table 2). In addition to the EC data, several other variables were also available. These included mensurational variables (e.g., mean diameter at breast height, DBH, and dominant tree height), soil properties (e.g., soil organic matter, texture, moisture profiles), energy balance terms (e.g., latent and sensible

Table 2
Supplementary site characteristics relating to data coverage, climate, leaf nitrogen, and EC data/processing

Site	Data[a]	Foliar nitrogen[b] (%)	u^*_{th} (m s^{-1})	Köppen climate code[c]	Total P in growing season (%)	Carbon balance terms (g C m^{-2} year^{-1})		Mean annual temperature (°C)		Total annual precipitation (mm)	
						P	F_{NEP}	2004 measured	LOCCLIM[d] 30-year normal	2004 measured	LOCCLIM 30-year normal
DF49	F	–	0.30	Cf	0.89	2562	113	8.77	9.24	1234	1374
EOBS	F	0.65	0.25	Dfb	0.91	593	17	0.28	−0.56	828	971
EPL	F	1.11	0.10	Dfb	0.96	656	108	5.34	5.88	914	894
F77	GS	0.95	0.25	Dfc	–	–	–	−1.48	−0.61	–	482
F89	GS	1.07	0.30	Dfc	–	–	–	−0.90	−0.23	–	454
F98	GS	1.35	0.35	Dfc	–	–	–	−0.13	0.35	–	411
FEN	F	–	0.10	Dfc	0.98	310	52	−0.40	0.42	576	450
GRS	F	1.60	0.25	BS	0.99	603	105	6.26	5.92	303	403
HBS00	F	–	0.15	Dfb	0.98	245	−144	0.04	−0.55	958	976
HDF00	F	–	0.08	Cf	0.98	762	−643	9.66	9.69	1365	1306
HDF88	F	–	0.16	Cf	0.95	1482	−212	10.17	9.68	1411	1370
HJP02	F	–	0.30	Dfc	0.75	73	−144	−0.93	0.83	–	448
HJP75	GS	–	0.20	Dfc	–	–	–	−0.16	0.40	–	448
NOBS	F	–	0.25	Dfc	0.96	580	42	−2.31	−2.62	379	520
OA	F	1.70	0.35	Dfc	1.00	860	1	0.76	0.50	489	403
OBF	F	1.10	0.40	Dfb	0.91	1120	611	3.94	4.52	–	1053
OJP	F	0.91	0.35	Dfc	0.85	551	−15	−0.23	0.39	491	448
OMW	F	–	0.30	Dfb	0.95	1013	157	1.93	1.90	685	813
SOBS	F	0.55	0.35	Dfc	0.87	688	19	0.76	0.04	543	431
WPL	F	1.31	0.20	Dfb	0.92	723	148	1.32	1.03	487	477
WPP02	S	–	0.10	Dfa	–	–	–	8.37	7.72	–	948
WPP39	F	–	0.35	Dfa	0.98	1367	205	7.87	7.81	956	950
WPP74	S	–	0.15	Dfa	–	–	–	8.31	7.81	–	952
WPP89	S	–	0.15	Dfa	–	–	–	8.17	7.75	–	948

Dashed entries indicate no data.

[a] Code meanings: F, complete 2004 data record, including gap filling and flux-partitioning for EC measurements; GS, EC data available only during the growing season, i.e., April–September, meteorological data available year around; S, sporadic non-uniform coverage, WPP02, WPP74, and WPP89 shared a roving eddy system with only <2 months data in the growing season, soil and several meteorological variables available year around or assumed the same as WPP39, e.g., PPT and S_t. Site-specific exceptions: HJP75, EC data coverage from May 1 to December 31, 2004, daily ε_g values were generated ($n = 27$) from gap filled EC data to cover the growing season only; F77, F89, F98, HJP02, HJP75, OBF, WPP02, WPP74, and WPP89, precipitation data too sparse in coverage or non-existent for a yearly total but daily values paired with growing season daily ε_g were available except for OBF (no data collected).

[b] Leaf nitrogen data were obtained between 2001 and 2005 from late June through mid-September, i.e., peak growing season values. Apart from GRS, no seasonal trajectories were available although some sites had replicate measurements spread out over a maximum of 1 month. Vegetation sampled was generally the dominant tree species. All measurement values available by site were averaged to obtain a canopy level value corresponding to the EC footprint. For GRS, the average per field measurement, c. every 14 d, was used for a seasonal trace.

[c] Köppen climate classification codes (http://www.fao.org/waicent/faoinfo/sustdev/EIdirect/climate/EIsp0002.htm) were based on 1961–1990 mean and monthly averages of MAT and mean and monthly totals of annual precipitation.

[d] LOCCLIM is a local climate estimator, which supports several interpolation methods, based on a worldwide network of 28,100 weather stations (http://www.fao.org/sd/2002/en1203a_en.htm). Thirty-year normals reference the 1961–1990 period. Shepard's interpolation method was used throughout.

heat), additional C balance terms (e.g., fine root productivity), foliage properties (e.g., foliar nitrogen [N]), ecological variables (e.g., ecozone, Köppen climate classification) and micrometeorological fields, including long-term normals (e.g., radiation variables, temperature, relative humidity, precipitation).

2.2. Calculation of light use efficiency

In this study, LUE is the ratio of daily or yearly P (g C m^{-2}) to daily or yearly absorbed PAR (Q_a, MJ m^{-2}, using 217 kJ mol^{-1} photons), hereafter: ε_g (g C MJ^{-1} Q_a). Using Q_a instead of incident or intercepted PAR serves to focus on the biological mechanism that drives P: a leaf responds to absorbed radiation, not incident or intercepted. In certain canopies, these three will be approximately equal. However, this requires sufficient LAI and canopy closure to ensure that most incoming radiation is absorbed. As the sites here ranged from open canopies with low LAI to closed canopies with high LAI this approach was rejected. Instead Q_a was determined using an adaptation of the Beer–Lambert law. Both Q_a and P were calculated for each half-hour and aggregated to daily or yearly values (ratio of totals).

The analysis of daily ε_g was limited to the growing season. This served as a quality control check on the EC data for the following reasons: (i) the number of gaps in winter data is larger than the growing season such that focusing on the latter reduces biases that may arise due to gap filling. (ii) The ability of coniferous systems to "switch on" during otherwise non-growing season periods is not well captured by EC data. All sites exhibited negative P fluxes, both daytime half-hourly and daily integrals, due to extrapolation issues with flux-partitioning (e.g., modeled daytime $R < |\text{measured } F_{NEP}|$ and $F_{NEP} < 0$), but their occurrence, while rare overall, increased outside of the growing season. (iii) Toward the tails of the growing season measured LAI, usually a single yearly value from the growing season, was compromised by dead foliage which degrades the $P \sim$ absorbed PAR relationship (Gower et al., 1999). The start of growing season was defined as the first day when a 5 d running average of mean daily air temperature at the height of the EC sensors exceeded 5 °C. The last day of the growing season occurred when this running mean went below the 5 °C threshold after summer solstice. For OA, a deciduous system, a daily trajectory of LAI was available (Barr et al., 2004). Here, the growing season is defined as any day when LAI $\neq 0$. For sites with a full yearly record of data, yearly ε_g values for the growing season and complete year are contrasted (Table 2).

P was calculated using a flux-partitioning procedure (Barr et al., 2004) based on friction velocity thresholds (u^*_{th}) as follows:

(i) Site-specific u^*_{th} were determined for each site using data from July–September. After the highest and lowest half percentiles of measured F_{NEP} (uncorrected for storage) were removed, F_{NEP} was then binned as a function of u^* using 10 bins of equal size. u^*_{th} was calculated using linear interpolation of u^* at 80% of the mean of F_{NEP} in the highest three bins. For GRS, this binning algorithm did not converge and a published value was used instead (Flanagan et al., 2002).

(ii) Nighttime F_{NEP} measured below this threshold as well as missing data were replaced by modeled values using a logistic function of near-surface soil temperature as the sole explanatory variable. This same function was used during the daytime to calculate R.

(iii) Missing daytime F_{NEP} was estimated with a Michaelis–Menten model using incident PAR. With daytime F_{NEP} and R known: $P = F_{NEP} + R$. Both the logistic and Michaelis–Menten functions were temporally localized within 100 point windows to capture seasonality (see Barr et al., 2004 for additional details).

This procedure is the standard used throughout. However, a linearized Q_{10} exponential model was also used to model R on a subset of sites. This resulted in a different estimate of P and allowed a quantification of the effects of flux-partitioning on ε_g.

All 24 sites included instrumentation to measure incident PAR (Q_o). Light was assumed to attenuate exponentially in the canopy with: $Q_a = \alpha_s Q_o(1 - e^{-kL^*})$, where α_s is canopy absorptivity: $1 - Q_u/Q_o$ or 0.95 in the absence of upwelling PAR (Q_u) measurements, and k is the extinction coefficient calculated half-hourly (Campbell and Norman, 1998, Eq. 15.4) as a function of solar zenith angle and leaf angle distribution (LAD). LAD was assumed either spherical, erectophile, or planophile (Table 1).

LAI was measured at each site using ground-based methods (Table 1) except for HJP02 and OBF where only the standard MODIS product was available. MODIS LAI (http://www.modis.ornl.gov/modis/modis_introduction.cfm) referenced only the pixel containing the tower. In most cases, only a single growing season value was available. Where multiple values throughout the year existed, a daily trajectory was created using polynomial-based interpolation. For sites located

in large tracts of homogeneous vegetation, e.g., NOBS, MODIS-based LAI was used to compare the effects of satellite-based versus ground-based LAI on ε_g. Q_a was also calculated using a fixed k of 0.5 or 0.7, corresponding to a typical range of measured values in extratropical forests (Chen et al., 1997; Aubin et al., 2000; Jarvis and Leverenz, 1983), to gauge the effects of different assumptions regarding canopy structure. Similarly, for some sites multiple ground-based LAI measurements were available. These were used to demonstrate the effects of differing measurement protocols and methods on ε_g.

2.3. Exploratory data analysis using tree regression

Regression trees were used to investigate relationships between daily ε_g and potential predictors. Such trees are built using recursive binary partitioning (Witten and Frank, 2005); a procedure that successively splits the data frame using a hierarchy of nodes, i.e., yes/no questions based on a value of a single predictor. This splitting criterion is chosen to best partition the data into homogenous groups. The topology of the tree can then be used to calculate the importance of each variable, i.e., variable selection. Variable importance is a normalized score from 0 to 100 where the most important predictor is given a score of 100. Regression trees, which are becoming more widespread in ecological research (e.g., De'ath and Fabricius, 2000; Lobell et al., 2005), are particularly suited to dealing with collinear predictors, outliers, and potentially insignificant predictors.

Tree regression, with ε_g as the response, was done for each biome to determine variable importance. The object was to rank variables in their capacity to explain the variation in daily ε_g. As such the predictor variables were primarily meteorological and direct inputs into the estimation of ε_g, such as Q_o, LAI, R, P, F_{NEP}, and near-surface soil temperature, were excluded.

Variables used were amplitude and mean of air temperature (T_{amp}, T_{air}) and vapor pressure deficit (D_{amp}, D), daytime Bowen ratio (β), mean daily sensible heat (H), latent heat flux (λE), net radiation flux (R_n), S_t and diffuse PAR (Q_d), the proportion of diffuse PAR in total PAR (p_{dif}), precipitation (both as an absolute value, PPT, and an indicator variable, I_{PPT}), and volumetric water content (θ). Both Q_d and p_{dif} were only available at six sites (five forested and one peatland). A separate tree was generated for the forested sites to quantify changes in variable importance due to the inclusion of diffuse radiation data. In addition to tree regression, univariate relationships between ε_g, important variables, depth to water table (for the two peatlands), and foliar N are discussed. Missing values, despite gap filling, were still present due to the failure of a specific instrument, the entire site being disabled, or a variable not being observed at a given site. At WPP74, WPP89, and WPP02 precipitation and S_t data were not recorded; data from nearby WPP39, the main chronosequence site, were used. Relative humidity, surface pressure, D, and PPT were not available for NOBS and values measured in Thompson, MB by Environment Canada (http://www.climate.weatheroffice.ec.gc.ca/climateData/canada_e.html) were used instead. For OBF, precipitation data were also not available and all analysis of OBF data excludes precipitation-derived variables. At GRS, NOBS, and OBF, total downwelling shortwave was not measured. For these sites, half-hourly S_t was estimated as a function of Q_o: $S_t = 0.6721 + 0.4952Q_o$, $r^2 = 0.99$, $p < 10^{-4}$, using all sites with a full year of both variables (cf. Meek et al., 1984). Soil moisture data were not available at FEN, HJP75, NOBS, and WPL and no suitable proxies were found; any analysis requiring θ necessarily excluded these four sites. After using these proxies, remaining gaps were not filled, beyond the flux-partitioning algorithm. For all exploratory data analyses any day with any missing value was not used.

Finally, an upper limit of ε_g (= 6.9124 g C MJ^{-1} Q_a based on the 8 photons required to fix 1 mol of CO_2; Bugbee and Monje, 1992) was also used. Daily ε_g values in excess of this value ($n = 15$) were deemed spurious and not included. It is noteworthy that limits on ε_g below the theoretical maximum based on biochemistry have been reported. Bugbee and Monje (1992) also discussed maximum ε_g values of c. 6.1 and 5 g C MJ^{-1} Q_a for laboratory and field conditions, respectively. Larcher (1995) suggested 2.5 g C MJ^{-1} Q_a as optimal in a natural setting. However, values in excess of these thresholds have been observed. Chen et al. (1999) reported daily ε_g values from a boreal deciduous forest up to c. 6 g C MJ^{-1} Q_a. Whitehead and Gower (2001) examined midsummer instantaneous ε_g of 11 plant species in Canada's boreal zone and reported values up to c. 7.2 g C MJ^{-1} Q_a. Similarly, lower limits have also been postulated. Ito and Oikawa (2004), in a global model-based study, reported maximum yearly ε_g of 1.2 g C MJ^{-1} Q_a. Reasons for these disparities are likely related to estimation method and spatio-temporal resolution. Of the 3466 site-days considered here only 276 had $\varepsilon_g > 2.5$ g C MJ^{-1} Q_a. While it is impossible to rule out estimation errors, these "high" values were retained for all analyses given the ambiguity in

constraining maximum ε_g below a biochemical upper limit.

2.4. Plant functional types

Daily ε_g values were compared on a site-by-site as well as PFT basis. Multiple sets of PFTs were defined using biome, ecozone, Köppen climate classification, chronosequence, and response surface. For a response surface PFT, normalized model fit results were passed to a *k*-means classifier (Everitt et al., 2001) with the optimal number of clusters, i.e., PFTs, determined following Krzanowski and Lai (1988). A single model was used: P regressed on Q_a using a Michaelis–Menten model where estimates of each parameter as well as goodness-of-fit metrics (r^2 and RMSE) were assumed to fully represent daily ε_g dynamics as well as quantifying how well-behaved, statistically, the representation was. In effect, the *k*-means generated clusters were a means to allow the data to self-organize with the possibility that the resulting PFTs could outperform those based on ecological variables.

2.5. Summarizing daily ε_g dynamics using regression techniques

As a means to summarize the daily dynamics of ε_g from c. 3500 site days across 24 sites and 3 biomes, we used multivariate linear regression with terms chosen based on variable importance. Two goodness-of-fit metrics were used, r^2 and RMSE, to quantify the adequacy of the resulting model-based summary and to test for functional convergence. Initially, the Yeo–Johnson family of transformations (Yeo and Johnson, 2000) was used to induce multivariate normality. Daily ε_g was then modeled using homogeneity of slopes for all 24 sites. Subsequently, PFT-based models were generated, i.e., a single PFT-wide intercept with the same terms as for the base model. We hypothesized that functional convergence occurs if goodness-of-fit metrics for a PFT-based model were comparable to site-specific ones based on the full model. Here, comparability was defined as a maximal 10% loss in r^2 relative to the highest site-specific value in a given PFT, $r^2 > 0.5$ overall, and no more than a 10% relative increase in RMSE.

2.6. Seasonality and yearly ε_g

As the growing season for all sites was not simultaneous, seasonality was tracked as a function of fractional thermal time. Growing season degree days (GDD), based on the 5 °C threshold used in delineating the growing season, were normalized to range from zero to unity. Daily ε_g was then smoothed, using a 15-point window, as a function of fractional GDD.

For yearly ε_g, the smaller number of data points resulted in a streamlined analysis. Only 17 sites had a complete year of EC data with 4 additional sites having a full growing season (Table 2). In addition to yearly meteorological values, several additional, e.g., mensurational, variables were also available. Yearly $\varepsilon_g \sim$ predictor relationships and the slope of a linear regression of yearly P on yearly Q_a (growing season and complete year) were used to summarize the dynamics of yearly ε_g. The regression was also used to test for convergence by evaluating the slope on a PFT-basis.

3. Results

3.1. Variable importance, selection, and univariate relationships

Variable importance varied by biome (Table 3). In general, site was of overriding importance in quantifying the variability of ε_g. The exception to this was the wetlands where the daily behavior of ε_g was similar across all sites. Beyond this a characterization of light (S_t), followed by temperature (T_{air}) were important predictors. For the five forested sites with measurements, diffuse PAR p_{dif}, a proxy for cloudiness, showed high importance. The ranking of water-related variables, i.e., λE, D, I_{PPT}, PPT, or θ, was more variable and generally much lower in importance score (<10) than temperature or light, apart from GRS where θ was critical.

Using light to characterize daily ε_g dynamics was supported by the curvilinear $P \sim Q_a$ relationship. In general, aggregating to longer time scales is thought to linearize this relationship (Ruimy et al., 1995). For daily ε_g at all sites a test of curvature, achieved by adding a quadratic term to a linear model, supported a curvilinear relationship ($p < 10^{-4}$). The model-based summary makes use of this artifact as a curvilinear relationship implies that ε_g varies with overall light levels. At some saturation level (= 10 MJ Q_a d^{-1} across all site days), a characterization of light becomes irrelevant. However, saturation levels were not regularly attained across the FCRN in 2004.

The relationships between any single variable and ε_g varied from site to site. Water table depth had little overall effect on ε_g for the peatlands (Fig. 1) although there was a range of water table depths at EPL where ε_g increased as the water table dropped. Similarly, foliar N

Table 3
Variable importance as determined using tree regression

Subset									
Forested sites with Q_d and p_{dif} measured ($n = 941$)		All forested sites with θ excluded ($n = 2513$)		All forested sites ($n = 2282$)		Grassland (GRS) ($n = 177$)		Wetlands with θ excluded (EPL, FEN, and WPL) ($n = 391$)	
Site	100	S_t	100	S_t	100	θ	100	β	100
S_t	77	Site	93	Site	95	D	48	S_t	92
p_{dif}	71	T_{air}	21	T_{air}	22	T_{air}	30	T_{air}	29
T_{air}	15	λE	8	λE	9	S_t	13	D_{amp}	10
θ	11			θ	4				

Regression trees were unpruned but limited to a maximum of 10 levels and a minimum 10 observations per node. Importance values, truncated to the nearest integer, are sorted by subset. Only variables with scores ≥10 and the highest ranked water-related (D, D_{amp}, I_{PPT}, λE, or PPT) are shown. θ is, if available, always shown. Q_d and p_{dif} were excluded from all trees except in the first column. Only sites with a full 2004 calendar year or the peak growing season were used. Each tree explained ≥87% of all variation in the data subset except for GRS where 74% was captured in the regression tree. This is analogous to the r^2 value from a 1:1 regression of observed on predicted ε_g values.

appeared to have no effect on the magnitude of peak growing season ε_g ($r^2 = 0.2$, $p = 0.26$, $n = 9$ forests). However, when repeated measurements were available, as for GRS, changes in foliar N, which decreased as the year progressed, were proportional to those in ε_g ($r^2 = 0.5$, $p < 0.02$). Daily ε_g was clearly enhanced by cloudiness (Fig. 2). When normalized for all six sites with Q_d measurements, mean daily ε_g increased linearly by a factor of 3 as p_{dif} increased from 0.1 to 1.0 (not shown). Univariate relationships for highly scored variables reflected their regression tree derived importance values with the caveat that a variable of high importance within a biome had variable explanatory power on a site-specific basis.

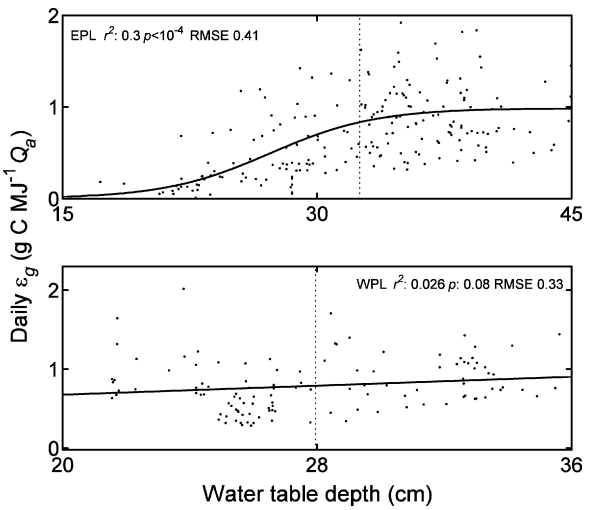

Fig. 1. Daily relationship between water table depth and ε_g during the 2004 growing season. Upper panel: EPL with a logistic curve superimposed. Lower panel: WPL and a linear fit. Dashed vertical line indicates mean water table depth.

3.2. Alternative daily ε_g calculations

Varying the calculation of Q_a, the source of LAI, or flux-partitioning method resulted in different ε_g values. For sites with higher LAI the difference in ε_g based on changes in calculating Q_a (i.e., a change in k or LAI) was negligible (e.g., DF49; $p = 0.98$ using the Kruskal–Wallis test (Hollander and Wolfe, 1999) across four alternative calculations of LAI) whereas for sites with sparser canopies a more noticeable change occurred (e.g., HBS00, $p < 0.01$ using $k = 0.5$ and 0.7 as alternatives). Varying the flux-partitioning model, i.e.,

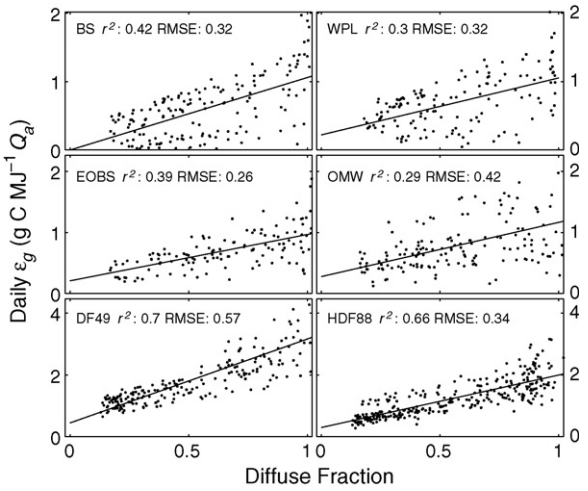

Fig. 2. Daily ε_g as a function of p_{dif} for all six sites where diffuse PAR measurements were available. Superimposed on all panels is a linear fit with goodness-of-fit statistics. As diffuse and total PAR were measured with different instruments the ratio of diffuse to total PAR exceeded unity in limited instances. These were generally at low light levels. Fit statistics were effectively unchanged irrespective of whether these points were included, excluded, or capped at unity.

changing from a logistic to exponential model of R and T_s, generally caused the distribution of ε_g to shift to the left; the mean decreased ($p = 0.002$, 0.19, and 0.01 for HDF00, HDF88, and DF49, respectively) with a negligible change in variability. Using MODIS LAI ε_g increased slightly. This effect was strongest during September and October, negligible otherwise and not significant (e.g., NOBS; $p = 0.31$). Overall, ε_g values were not sensitive to changes in calculation procedures as evidenced by the large amount of overlap between distributions of ε_g for the different calculation methods (not shown).

3.3. Toward a model-based summary of daily radiation use efficiency

Given the variable rankings and data availability constraints, the base model consisted of T_{air} and S_t. As water relations, despite showing marginal importance here, are generally assumed to be important considerations regarding the dynamics of ε_g (e.g., Allen et al., 2005; Green et al., 2003; McMurtrie et al., 1994; Potter et al., 1999; Ruimy et al., 1999; Runyon et al., 1994; Whitehead and Beadle, 2004), the most important water-related variable, λE, was also included. This resulted in two models (one with and one without λE) where each assumed homogeneity of slopes, i.e., each site ($n = 24$) had a unique intercept. These two models explained 75–77% of the variation in daily ε_g. The cost of excluding the most important water-related variable, λE, was negligible. Its exclusion, despite statistical significance ($p < 10^{-4}$), resulted in an additional c. 2% loss in explanatory power with a <0.01 g C MJ^{-1} Q_a loss in precision. Based on the overall performance of using just T_{air} and S_t only this model is considered further (Table 4).

On a site-specific basis, the base model explained variation in ε_g with varying degrees of success for most ($n = 17$) sites (Table 4; $0.50 \leq r^2 \leq 0.77$). For five sites (HDF00, HJP02, OA, OMW, and WPP74), the base model provided only marginal explanatory power ($0.22 \leq r^2 \leq 0.49$). For GRS, the model lacked any usefulness ($r^2 < 0.01$). Using tree regression on those sites with complete growing season data led to increases in explanatory power ($0.74 \leq r^2 \leq 0.89$) and highlighted the importance of variables missing from the base model (Table 5). Specifically, variables related to the energy balance (β, R_n, and H), vapor deficit (D_{amp}, D), and soil water (θ) consistently appeared in the regression trees. The pattern of these variable importance scores suggests that the coupling of meteorological drivers at these sites is different from the transect as a whole.

Table 4
Site-specific fit results using base linear regression model

Site	I_{Site}	r^2	RMSE
DF49	1.294	0.77	0.16
EOBS	0.770	0.64	0.12
EPL	0.786	0.65	0.17
F77	1.021	0.73	0.16
F89	1.230	0.66	0.22
F98	0.851	0.66	0.18
FEN	0.777	0.50	0.21
GRS	1.814	0.01	0.39
HBS00	0.767	0.55	0.22
HDF00	0.728	0.22	0.27
HDF88	0.999	0.74	0.14
HJP02	0.434	0.22	0.08
HJP75	0.763	0.67	0.11
NOBS	0.838	0.69	0.18
OA	1.077	0.42	0.21
OBF	0.996	0.56	0.18
OJP	0.728	0.62	0.15
OMW	0.901	0.26	0.24
SOBS	0.777	0.71	0.15
WPL	0.828	0.60	0.15
WPP02	1.063	0.52	0.31
WPP39	1.042	0.55	0.21
WPP74	0.721	0.49	0.32
WPP89	1.330	0.64	0.21

All terms highly significant ($p < 10^{-4}$). I_{Site} is an indicator variable that maps each site to a site-specific intercept. Normalizing Yeo–Johnson transformations by site were performed on ε_g and S_t leading to the following base model: $\log(\varepsilon_g) = I_{Site} - 0.00993 \cdot S_t^{0.73} + 0.01927 \cdot T_{air}$, $r^2 = 0.75$; RMSE = 0.21; $n = 3466$. The Yeo–Johnson transformation for S_t is $y^* = ((y+1)^{\lambda} - 1)/\lambda$, and $y^* = \log(y+1)$ for ε_g, where λ (= 0.73) indicates the transformation parameter (shown as superscript), y the untransformed data, and y^* is the transformed data used in regression analysis.

Extending this base model to PFTs degraded model performance relative to site-specific runs (Table 6). In general, model performance and the number of sites per PFT were inversely related and the overall performance

Table 5
Important variables (score ≥ 10) in descending order as determined by tree regression with a maximum of 10 levels and a minimum of 10 observations per node

Site	Important variables	Explanatory power
GRS	θ, D, T_{air}, S_t	0.74
HDF00	T_{amp}, T_{air}, R_n, S_t, θ, β, λE	0.84
HJP02	R_n, T_{amp}, θ, λE, D	0.87
OA	S_t, β, θ, PPT	0.89
OMW	β, S_t, θ, D, λE, T_{air}, H	0.87

For the sites included ($n = 5$) the base model performed poorly indicating that additional variables were needed to better model daily ε_g dynamics. Explanatory power was computed from a 1:1 regression of observed on predicted values.

Table 6
Explanatory power of base linear regression model by PFT with a common intercept

PFT		r^2	RMSE
Method	Site information		
k-means using fit results from $P \sim Q_a$, forested sites	$n = 11$	0.42	0.27
	$n = 6$	0.31	0.30
k-means using fit results from $P \sim Q_a$, all sites	$n = 11$	0.50	0.23
	$n = 5$	0.43	0.29
	$n = 4$	0.01	0.55
	HBS00	0.59	0.21
Biome	Wetlands (EPL, FEN, WPL)	0.68	0.16
	Grassland (GRS)	0.01	0.39
	Forests ($n = 20$)	0.36	0.31
Ecozone (only forested sites)	Boreal coniferous ($n = 10$)	0.42	0.27
	Boreal deciduous (OA)	0.42	0.21
	Maritime coniferous forest ($n = 4$; *P. menziesii* chronosequence and OBF)	0.29	0.32
	Temperate forest ($n = 5$; OMW and *P. strobus* chronosequence)	0.41	0.28
Köppen classification	BS (GRS)	0.01	0.33
	Cf ($n = 3$; *P. menziesii* chronosequence)	0.26	0.34
	Dfa ($n = 4$; *P. strobus* chronosequence)	0.50	0.27
	Dfb ($n = 6$)	0.46	0.21
	Dfc ($n = 10$)	0.41	0.28
Chronosequence	*P. menziesii*: HDF00, HDF88, DF49	0.26	0.34
	P. banksiana after harvest: HJP02, HJP75, OJP	0.32	0.21
	P. strobus: WPP02, WPP89, WPP74, WPP39	0.50	0.27
	P. mariana toposequence: EOBS, HBS00, NOBS, SOBS	0.64	0.17
	P. banksiana after burn: F98, F89, F77	0.55	0.26

All regression models were highly significant ($p < 10^{-4}$). k-Means PFTs were determined using normalized Michaelis–Menten model results for either forested ($n = 17$) or all sites ($n = 21$) with at least full growing season coverage.

was poor ($r^2 < 0.5$). As an exception, for wetlands the PFT-based model showed superior performance relative to the individual three sites. Also, the *Picea mariana* toposequence exhibited convergence. For the fire *Pinus banksiana* and *Pinus strobus* chronosequences PFT-based performance was adequate ($0.5 \leq r^2 \leq 0.55$) but insufficient for convergence (change in RMSE too high). Using boundary line analysis based on site-specific maximum ε_g, S_t, T_a, and λE (not shown) resulted in worse performance ($r^2 \leq 0.36$ across all sites and PFTs).

3.4. Seasonality and magnitude of daily ε_g

The time series of daily ε_g was highly variable with little in common between sites. For the 17 sites with a data record for all of 2004, peak ε_g by site was achieved between mid-August and mid-September with the mixed-grass prairie (GRS) and the 2 younger coniferous temperature rainforests (HDF00 and HDF88) having maximum daily ε_g toward the beginning of the growing season, before May. In general, boreal sites tended to have lower peak (and median) values than non-boreal sites (Table 7). However, these peaks were episodic. Expressed as function of fractional thermal time, and smoothed using a 15-point moving average to remove short-term episodic events, daily ε_g increased during the course of the growing season with peak values occurring at c. >0.80 of total thermal time for 2004 (Fig. 3). This trend held for all sites except FEN (Fig. 3) and GRS (not shown), which peaked earlier (fractional thermal time <0.45). Post-peak behavior of ε_g was variable with either a steady decrease toward non-growing season levels or, after a pronounced trough, a secondary peak as the growing season ended. Across the full year most (92%) daily values were less than 2.5 g C MJ^{-1} Q_a for both forests and wetlands with the highest values, at DF49, GRS, F89, and WPP02

Table 7
Summary of daily and yearly ε_g (g C MJ^{-1} Q_a) by site and biome in 2004

Site/biome	Daily ε_g		Yearly ε_g	
	Median	Maximum	Full year	Growing season
DF49	1.63	6.69	1.59	1.59
EOBS	0.66	1.88	0.41	0.63
EPL	0.69	2.90	0.53	0.61
F77	0.91	4.72	–	0.86
F89	1.54	6.37	–	1.39
F98	0.63	3.51	–	0.61
FEN	0.59	2.33	0.41	0.56
GRS	3.67	6.87	3.64	3.64
HBS00	0.70	3.35	0.48	0.62
HDF00	0.62	2.95	0.70	0.70
HDF88	1.17	3.16	0.95	0.92
HJP02	0.11	0.66	0.09	0.10
HJP75	0.48	1.69	–	0.43
NOBS	0.75	3.14	0.41	0.66
OA	1.28	3.07	1.24	1.24
OBF	0.91	4.62	0.83	0.94
OJP	0.50	1.79	0.39	0.45
OMW	0.72	3.29	0.60	0.79
SOBS	0.58	1.97	0.43	0.51
WPL	0.67	2.02	0.51	0.62
WPP02	1.02	6.59	–	–
WPP39	1.17	5.89	0.95	1.11
WPP74	0.40	2.09	–	–
WPP89	1.90	3.80	–	–
Forest	0.84	6.69	0.60	0.70
Grassland	3.67	6.87	3.64	3.64
Wetland	0.65	2.90	0.51	0.61

Dashed entries indicate no data.

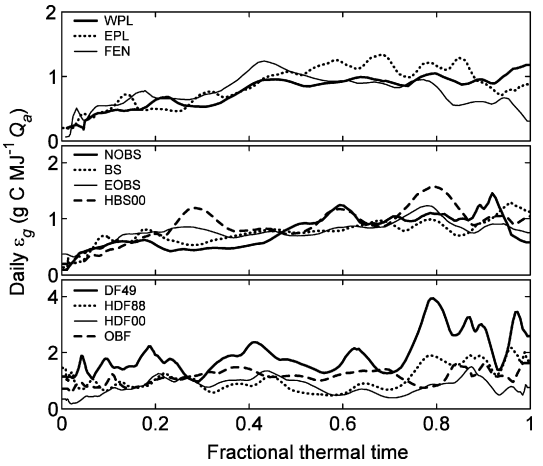

Fig. 3. Seasonal progression of ε_g as a function of fractional thermal time during the growing season. Top panel: wetlands; middle panel: the *P. mariana* toposequence; and lower panel: the coniferous–maritime ecozone. Fractional thermal time is the summation of growing degree days above a 5 °C threshold used to define the growing season. These values were then normalized to [0,1]. Daily ε_g was subsequently smoothed using a 15-point moving average as a function of fractional thermal time.

exceeding 6 g C MJ^{-1} Q_a. In general, the lone grassland (GRS) was the most efficient in converting light into photosynthates followed by forested sites and finally wetlands, although there was considerable distributional overlap between the latter two biomes (not shown).

3.5. Yearly ε_g

Yearly values of ε_g were lowest in coniferous boreal forests and wetlands, intermediate in more temperate climates and at OA, a coniferous boreal forest; and highest in the lone grassland (Table 7) with growing season $\varepsilon_g \geq$ full year ε_g. Despite the large number of potential predictors, univariate relationships with significant explanatory power for yearly or growing season ε_g were limited to mean annual temperature (MAT) and yearly maximal LAI. The additional variables unavailable in the daily context (e.g., mensurational, topographical, and 30-year normals) were not useful by any standard. Initially, biome-specific relationships were investigated. However, the similarity between forested and wetland sites resulted in these being aggregated into a single grouping. Only GRS, a clear outlying value, was not included in model fitting (Fig. 4). The outliers OA and DF49 did not unduly influence the fit and were retained. Furthermore, the relationships were best expressed using ε_g for the entire year. For LAI, model fit results were effectively unchanged in either case. For MAT, restricting the time period to the growing season collapsed the distribution of MAT resulting in a large degradation in goodness-of-fit. Combining these two terms yielded a linear base model for yearly ε_g with medium explanatory power ($r^2 = 0.56$; Fig. 4).

In the feature space defined by yearly or growing season totals of P and Q_a, functional convergence occurred using all D Köppen sites, i.e., all sites except the grassland (GRS) and the *Pseudotsuga menziesii* chronosequence, for the growing season as well as for the entire year, albeit weaker (Fig. 5). Yearly ε_g (mean ± standard error) was 0.56 ± 0.08 g C MJ^{-1} Q_a for the full year and slightly higher (0.71 ± 0.08 g C MJ^{-1} Q_a) for the growing season. Using the regression slopes (Fig. 5) gave similar values: 0.53 ± 0.20 g C MJ^{-1} Q_a for the full year and 0.70 ± 0.20 g C MJ^{-1} Q_a for the growing season. This implies that the three wetlands, which all share the D Köppen classification, share a single ε_g value as well.

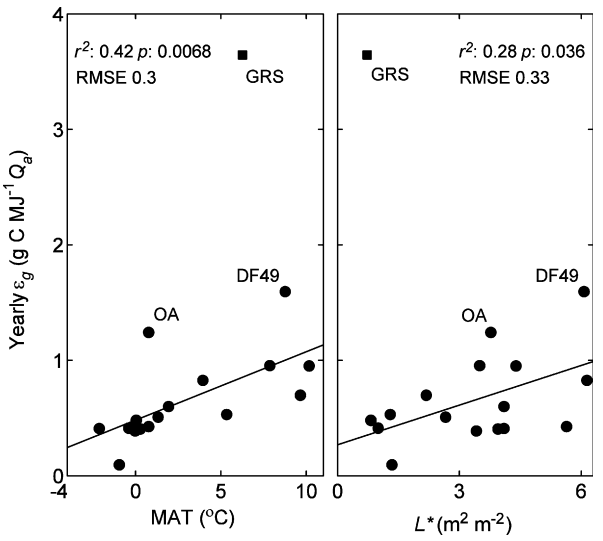

Fig. 4. Yearly ε_g as a function of mean annual temperature (MAT, °C) and maximum LAI. Only the sites with a full yearly data record are shown ($n = 17$). Solid line shows linear fit excluding GRS (solid square). Individually labeled sites (solid circles) have medium leverage on the regression line. Using both predictors yielded a simple model of yearly ε_g for wetlands and forests: $y = 0.2177 + 0.0505 \cdot \text{MAT} + 0.0852 \cdot L^*$, with $r^2 = 0.56$, $p < 0.005$, and RMSE = 0.27.

For all forested sites, this was not the case. DF49 is a clear outlying value (Cook's distance = 0.97 (Cook and Weisberg, 1999) for DF49 and <0.13 for other forested sites in the growing season), particularly due to its large annual P. In contrast to GRS, the only grassland and only site with a BS Köppen classification, why DF49 should be excluded is more ambiguous. DF49 had the highest total annual P, the fifth highest total F_{NEP}, the third highest mean annual temperature, and the third largest LAI (Tables 1 and 2). Sites ranked higher in all but annual P totals were not outliers, and nor were the site history or other site characteristics unique. The other two sites in the *P. menziesii* chronosequence, where variation in C cycling is assumed to be primarily a function of age, were not outlying values. In the absence of a valid reason to exclude DF49, the linear relationship indicative of functional convergence for all forested sites is untenable. It is plausible that C Köppen classified sites have different trade-offs between P and Q_a but that these could not be statistically captured due to the small sample size ($n = 3$).

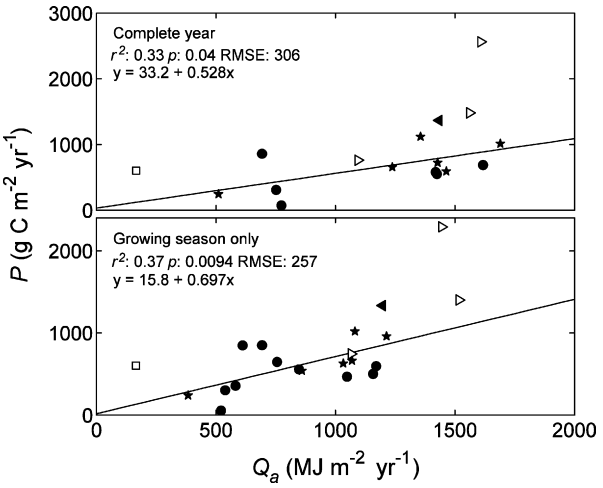

Fig. 5. Linear regressions of P on Q_a for the complete year (upper panel, $n = 17$) and the growing season only (lower panel, $n = 21$). Sites are label according to Köppen code: BS (open square), Cf (open triangle), Dfa (solid triangle), Dfb (solid star), and Dfc (solid circle). Fitted lines are based on Köppen D sites only (solid symbols). Tests of curvature ($p = 0.74$ and 0.89 for upper and lower panels) support a linear relationship. The slope of the regression line is an unbiased estimate of yearly ε_g for the Köppen D sites used in fitting.

The variability in yearly ε_g values due to calculation method was modest. For DF49, all values were <0.02 g C MJ^{-1} Q_a (<2%) from the base value, except the yearly value based on an alternative flux-partitioning method. Here, this discrepancy was 0.18 g C MJ^{-1} Q_a (c. 11%). For NOBS, the two alternative values were c. 0.035 g C MJ^{-1} Q_a apart. Similar to the daily time scale, variability was more pronounced at sites with sparser canopies. For example, yearly values at HBS00 were 0.62, 0.87, and 0.67 g C MJ^{-1} Q_a for the base, $k = 0.5$, and $k = 0.7$ alternatives, respectively.

4. Discussion

4.1. Intercomparison of estimates of ε_g

Ideally, an intercomparison of EC-derived estimates of LUE would show broad agreement with the values presented here or highlight trends. However, the bulk of studies examining LUE use NPP in the numerator (i.e., calculate ε_n), generally obtained through C stock studies with P unreported. While it is tempting to apply a C use efficiency (CUE) of 0.5 to convert from ε_n to ε_g this was deemed inappropriate. There is much empirical evidence that 0.5 is a very rough estimate (Amthor, 2000). For example, annual CUE values for forested ecosystems as reported in Gifford (2003) and Ryan et al. (1997) vary from 0.35 (boreal forest) to 0.55 (temperate forest). Age-linked changes in CUE have also been postulated (e.g., Mäkelä and Valentine, 2001). Furthermore, the theoretical justification for functional convergence of ε_g is based on variable autotrophic respiration that scales with P (Goetz and Prince, 1999).

EC-based estimates of ε_g are typically based on half-hourly data (e.g., Gu et al., 2002). In this case the

$P \sim Q_a$ relationship is curvilinear (Ruimy et al., 1995). The metric reported, quantum yield, is the slope at the origin and would be comparable to ε_g as reported here after temporal scaling and if the response were linear (i.e., maximum $P \rightarrow \infty$). Quantum yield does not characterize LUE over any defined time period whereas ε_g is a ratio of totals referenced to a day or year.

Some studies using half-hourly data do offer points of comparison. Nichol et al. (2000, 2002) used half-hourly EC measurements obtained under certain sky conditions to create a ratio comparable to ε_g estimates given here. Over four different canopies in the Siberian boreal forest (60.75°N, 89.38°E, 80 m a.s.l.) ε_g, calculated using Q_o and the ratio of averages from 1230 to 1430 h, ranged from 0.001 to 0.006 mol CO_2 mol^{-1} photons or 0.055–0.33 g C MJ^{-1} Q_o during the winter–spring transition (Nichol et al., 2002). Using BOREAS data from May through September 1994, Nichol et al. (2000) calculated ε_g, defined as in the Siberian forest but for clear days only ($Q_o > 900$ μmol), at FEN, OA, OJP, and SOBS. These values ranged from 0.001 to 0.01 mol CO_2 mol^{-1} photons or from 0.055 to 0.55 g C MJ^{-1} Q_o and were comparable with the range of values for the forested biome in general and boreal sites in particular (Table 7). The slight bias toward smaller values in Nichol et al. (2000, 2002) is likely a result of the measurement time: ε_g was measured close to solar noon (±2 h) and under clear skies, conditions that are associated with less efficient conversion of absorbed PAR into photosynthates. Furthermore, when LAI is low, using Q_o in the denominator leads to an underestimate relative to ε_g in this study, i.e., $Q_o > Q_a$.

Chen et al. (1999) calculated daily photosynthetic energy use efficiency relative to Q_a for 1994 and 1996 at OA and found values ranging from c. 1 to 22% or, expressed as daily ε_g using 479 kJ mol^{-1} CH_2O in stored carbohydrates, c. 0.05 to 6 g C MJ^{-1} Q_a. 2004 values were (0.2–3.1 g C MJ^{-1} Q_a) within this range. The larger values ($\varepsilon_g > 3$ g C MJ^{-1} Q_a) reported by Chen et al. (1999) were rare (<10 d in both 1994 and 1996) and related to air temperature: mean T_{air} from DOY 150 to 250 (roughly the peak growing season) was 15.0, 16.3, and 13.7 °C for 1994, 1996, and 2004. In addition to daily values, Chen et al. (1999) reported yearly photosynthetic energy use efficiency values, after adjusting for periods where LAI = 0, of 5.0 and 4.6% in 1994 and 1996. This corresponds to 1.25 and 1.15 g C MJ^{-1} Q_a, respectively, and is in good agreement with the value for 2004, 1.24 g C MJ^{-1} Q_a.

Finally, Turner et al. (2003b) analyzed daily and monthly ε_g at four EC sites, including NOBS and a site comparable to GRS with 1997 data, and found growing season (June–September) mean daily ε_g of 1.0 for NOBS and 1.7 g C MJ^{-1} Q_a for a tall grass prairie (Konza Long Term Ecological Research Station, 39.08°N, 96.56°W, 393 m a.s.l.). The NOBS values reported here ranged from 0.1 to 3.1 g C MJ^{-1} Q_a with a yearly mean daily ε_g value of 0.9 g C MJ^{-1} Q_a. The GRS site (mean daily ε_g = 3.6 g C MJ^{-1} Q_a), however, was more efficient than the grassland at Konza. While interannual variability (Nouvellon et al., 2000), climate, and vegetation certainly play a role in explaining the 200% relative difference within a single biome or PFT (GRS versus Konza), this variability highlights the uncertainty in ε_g in general (Lagergren et al., 2005) and underscores the need to more accurately characterize ε_g dynamics for modeling purposes.

4.2. Ecological insights

The advent of chronosequence EC studies has enabled the investigation of succession, i.e., age, on C cycling. Included in the 24 sites used were 3 chronosequences. The *P. strobus* chronosequence was excluded in this context due to the skewed data distribution: c. 70% of all data points were from WPP39 and three of the four sites lacked a full growing season. However, no age-related trends that spanned all three, whether limited to daily, yearly growing season, or full yearly ε_g values, were discernable. All measures of ε_g for the fire *P. banksiana* chronosequence were ranked, from largest to smallest, F89, F77, and F98, i.e., peak behavior was exhibited in the middle-aged stand. The other two chronosequences, *P. menziesii* and harvested *P. banksiana*, showed progressively higher ε_g with age (Table 7). As these trends diverge, an age-related signal in ε_g was not found. It is noteworthy that ε_g at F77 is roughly twice that of HJP75. Although these sites are geographically quite close and similarly aged, it is not clear that this difference is caused by the treatment effect, i.e., fire versus harvesting, or by local site differences.

In contrast to studies showing a linkage between foliar N and LUE (e.g., Boegh et al., 2002; Medlyn, 1996) no relationship was found in the FCRN sites for 2004, apart from GRS where a seasonal trajectory of foliar N was available. This is potentially related to issues of data coverage. Foliar N was measured only at a subset of sites without uniform temporal coverage, although at least one measurement during the peak growing season was the desired target. Furthermore, the measurements were not in 1:1 correspondence with the vegetation in the eddy flux footprint. In most cases, values were for dominant tree species only. All this was

reflected in the difficulties in matching ε_g with the data available. It is noteworthy that the linkage between foliar N and LUE has been hypothesized primarily using ε_n data. The lack of correlation in this study may be an expression of variable autotrophic respiration (sensu Goetz and Prince, 1999). Alternatively, at continental scales, the importance of foliar N could be marginalized by that of light and temperature.

More so than for foliar N, the lack of explanatory power of water-related variables was unexpected. Water relations have long been implicated as a strong controlling force on LUE. The weight of evidence in this study supports that water relations had negligible impact in explaining the dynamics of ε_g across this transect in 2004:

(1) Biome-specific variable importance scores, with daily ε_g as the response, of any water-related variable were low with the most important water-related variable, λE, having only negligible importance (Table 3) except at GRS. This is in contrast to the presence of episodic water stress events, i.e., <7 d with low θ, minimal rainfall, high T_{air}, and water deficits. These events occurred in August or September and depressed ε_g, but were not sufficient to warrant the inclusion of water-related variables in any model-based summary for the transect. Furthermore, of the sites not well predicted by the base model site-specific regression trees did not show consistently highly scored water-related variables (Table 5).
(2) Comparing overall water inputs in 2004 is also instructive. The longest maintained site has existed for <15 years so 1961–1990 normals, interpolated using Shepard's method from LocClim (http://www.fao.org/sd/2002/en1203a_en.htm), were used instead. For $n = 10$ of 15 sites with complete 2004 precipitation data, 30-year normals were less than measured precipitation (Table 2), indicating a surplus of water inputs into the system. Of the five sites with a water deficit, only OMW was not well predicted by the base model but a site-specific regression tree did not show highly scored water-related variables (Table 5). There is some uncertainty in the 30-year normals that arise from spatial interpolation procedures but given the quality of the database used for interpolation ($n = 28{,}100$ weather stations with good coverage in the lower part of Canada), the probability that the 30-year normals presented here do not adequately characterize long-term site precipitation trends must be viewed as small.

This suggests that the network, as a whole, was effectively drought free during 2004. However, hydrological influences on ε_g are not limited to periods of water stress. The denominator of ε_g is largely unaffected by changes in water relations except in the event of severe drought and concomitant loss of effective LAI. The numerator, P, is linked to water relations though its interdependencies with stomatal conductance and the biochemistry of photosynthesis itself. Given this context, the redundancy of water-related variables in modeling ε_g could be caused by longer-term acclimation processes. The vegetation at each site is natural. Despite some planted stock the existent assemblages are within the realm of vegetation communities that would exist in the absence of management. The exception to this is the *P. strobus* plantation chronosequence. But even in this case *P. strobus* occurs naturally in southern Ontario, albeit not in monocultures. In effect, the vegetation has acclimatized to prevailing hydrological conditions through biogeography such that only years widely divergent from prevailing long-term trends, e.g., a 100-year drought, would cause water relations to be important in describing the variability of ε_g beyond light and temperature relations.

4.3. Functional convergence, plant functional types, and implications for modeling

Apart from the wetlands biome and *P. mariana* toposequence PFTs no sign of convergence was found. Instead, aggregation using PFTs was penalized by a severe loss in model performance. This was in opposition to strong theoretical arguments supporting convergence in ε_g (Goetz and Prince, 1999). For yearly values of ε_g convergence was more plausible using a broad climate classification. The existence of within-PFT convergence was not altered using ε_g values based on different flux-partitioning methods, measurement techniques, or canopy structural assumptions, nor were other results significantly modified.

The general lack of convergence at the daily time step and increasing conservative behavior at the yearly time step for ε_g imply that convergence at the footprint scale is related to temporal scaling, i.e., the longer the scaling interval the more likely this desirable conservative behavior occurs. Implications for production efficiency models using PFT-based LUE values at finer temporal scales (e.g., Veroustraete et al., 2004) include: (i) a large loss of predictive power, (ii) the inability to capture the full range of dynamics, and (iii) better model performance with longer time steps. Nonetheless, spatial scaling may act to counterbalance this. For

example, Mahrt and Vickers (2002) found that, using BOREAS data and companion aircraft-based flux measurements, area-averaged half-hourly water vapor and C fluxes were more stable than from individual EC sites. Here, stability was defined as less scatter and more meaningful, in a statistical sense, relationships between area-averaged fluxes and forcing variables. The averaging area used, from the BOREAS southern study area, comprised water features, wetlands, burned areas, coniferous and deciduous forests, or at least three PFTs given the definitions used here based primarily on vegetation.

In sum, our results appear to invalidate the idea that a constant ε_g value can be applied across sites, particularly using daily values. Further research is needed to better understand why LUE is so variable across sites, e.g., why is ε_g so much higher at DF49, F89, GRS, and WPP02 than at other sites? It must be noted that the ultimate test of conservative ε_g behavior relates to the use of such estimates, i.e., what is sufficiently conservative for a continental-scale application may not be suitable for finer scaled applications. Lastly, the dependency of conservative LUE behavior on spatio-temporal scale holds promise for modeling frameworks. A production efficiency model based on the scale where convergence is maximized would result in better overall performance.

5. Conclusions

(1) Daily ε_g in 2004 was highly variable across the FCRN both spatially and temporally. In general, daily and yearly ε_g values for coniferous boreal systems were less than in more temperate systems, including the lone deciduous boreal system. The grassland was the most efficient site (daily median $\pm$ interquartile range: 3.68 ± 1.98 g C MJ^{-1} Q_a) at converting absorbed PAR into photosynthates, followed by forests (0.84 ± 0.82 g C MJ^{-1} Q_a) with wetlands (0.65 ± 0.54 g C MJ^{-1} Q_a) being the least efficient. Daily ε_g generally exhibited a weak peak toward the end of the growing season. Yearly ε_g values ranged from 0.1 to 3.6 g C MJ^{-1} Q_a overall with relative rankings similar to daily values.

(2) Daily dynamics of ε_g in 2004 across the transect were driven by light and temperature to the exclusion of water-related variables. Similarly, foliar N was not a useful predictor except for the repeated measures available at GRS. Cloudiness, p_{dif}, was an important covariate in the subset of sites ($n = 6$) for which it was available, suggesting the usefulness of cloud cover data in modeling daily ε_g. For yearly ε_g values, only MAT and LAI were useful covariates.

(3) A conservative behavior of daily ε_g using PFTs was not evident. Only the three wetland sites and the four sites in the *P. mariana* toposequence could be aggregated in the context of functional convergence. This invalidates the use of conservative PFT-wide ε_g values in modeling contexts, particularly on shorter time scales. For yearly values, convergence was more apparent and linked to Köppen climate classification.

Acknowledgements

Funding for this research was provided by the Fluxnet Canada Research Network (FCRN), Canadian Foundation for Climate and Atmospheric Sciences (CFCAS), and BIOCAP Canada Foundation for CRS; and a Natural Science and Engineering Research Council of Canada (NSERC) Operating Grant for TAB. Additional funding was provided by the B.C. Ministry of Forests, the Canadian Forest Service, the Meteorological Service of Canada, Parks Canada, and the U.S. National Aeronautics and Space Administration. Ancillary data was provided by Pierre Bernier, Roger Cox, and Xinbiao Zhu (Canadian Forest Service) as well as Onil Bergeron, Natalia Restrepo-Coupe, Andrea Eccleston, Ajit Govind, Matthew Regier, and Zisheng Xing (graduate students). We also thank the numerous technicians, students, and research fellows that contributed to data collection and processing. Finally, the helpful comments of Helen Cleugh and two anonymous reviewers are acknowledged.

References

Aalto, T., Ciais, P., Chevillard, A., Moulin, C., 2004. Optimal determination of the parameters controlling biospheric CO_2 fluxes over Europe using eddy covariance fluxes and satellite NDVI measurements. Tellus B 56 (2), 93–104.

Ahl, D.E., Gower, S.T., Mackay, D.S., Burrows, S.N., Norman, J.M., Diak, G., 2004. Light use efficiency of a heterogeneous forest in northern Wisconsin: implications for remote sensing and modeling net primary production. Remote Sens. Environ. 93, 168–178.

Allen, C.B., Will, R.E., McGarvery, R.C., Coyle, D.R., Coleman, M.D., 2005. Radiation-use efficiency and gas exchange responses to water and nutrient availability in irrigated and fertilized stands of sweetgum and sycamore. Tree Physiol. 25, 191–200.

Amthor, J.S., 2000. The McCree-de Wit-Penning de Vries-Thornley respiration paradigms: 30 years later. Ann. Bot. 86, 1–20.

Aubin, I., Beaudet, M., Messier, C., 2000. Light extinction coefficients specific to the understorey vegetation of the southern boreal forest. Quebec: Can. J. For. Res. 30, 168–177.

Barr, A.G., Black, T.A., Hogg, E.H., Kljun, N., Morgenstern, K., Nesic, Z., 2004. Inter-annual variability in the leaf area index of a boreal aspen-hazelnut forest in relation to net ecosystem production. Agric. For. Meteorol. 126 (3–4), 237–255.

Boegh, E., Soegaard, H., Broge, N., Hasager, C.B., Jensen, N.O., Schelde, K., Thomsen, A., 2002. Airborne multispectral data for quantifying leaf area index, nitrogen concentration, and photosynthetic efficiency in agriculture. Remote Sens. Environ. 81 (2–3), 179–193.

Bugbee, B., Monje, O., 1992. The limits of crop productivity. Bioscience 42 (7), 494–503.

Campbell, G.S., Norman, J.M., 1998. An Introduction to Environmental Biophysics, second ed. Springer Verlag, 286 pp.

Chen, D.X., Coughenour, M.B., 2004. Photosynthesis, transpiration, and primary productivity: scaling up from leaves to canopies and regions using process models and remotely sensed data. Global Biogeochem. Cycles 18 (4), GB4033.

Chen, J.M., Blanken, P.D., Black, T.A., Guibeault, M., Chen, S., 1997. Radiation regime and canopy architecture in a boreal aspen forest. Agric. For. Meteorol. 86, 107–125.

Chen, W.J., Black, T.A., Yang, P.C., Barr, A.G., Neumann, H.H., Nesic, Z., Blanken, P.D., Novak, M.D., Eley, J., Ketler, R.J., Cuenca, R., 1999. Effects of climatic variability on the annual carbon sequestration by a boreal aspen forest. Global Change Biol. 5 (1), 41–53.

Cramer, W., 1997. Using plant functional types in a global vegetation model. In: Smith, T.M., Shugart, H.H., Woodward, F.I. (Eds.), Plant Functional Types: Their Relevance to Ecosystem Properties and Global Change, vol. 1. Cambridge University Press. IGBP Book Series, Cambridge, pp. 271–288.

Cramer, W., Kicklighter, D.W., Bondeau, A., Moore III, B., Churkina, G., Nemry, B., Ruimy, A., Schloss, A.L., Participants of the Potsdam NPP Model Intercomparison, 1999a. Comparing global models of terrestrial net primary productivity (NPP): overview and key results. Global Change Biol. 5 (Suppl. 1), 1–15.

Cramer, W., Shugart, H.H., Noble, I.R., Woodward, F.I., Bugmann, H., Bondeau, A., Foley, J.A., Gardner, R.H., Lauenroth, B., Pitelka, L.F., Sala, O., Sutherst, R.W., 1999b. Ecosystem composition and structure. In: Walker, B.H., Steffen, W.L., Canadell, J., Ingram, J.S.I. (Eds.), The Terrestrial Biosphere and Global Change: Implications for Natural and Managed Ecosystems, vol. 4. Cambridge University Press. IGBP Book Series, Cambridge, pp. 190–228.

Cook, R.D., Weisberg, S., 1999. Applied Regression Including Computing and Graphics. Wiley–Interscience, New York, NY, 632 pp.

De'ath, G., Fabricius, K.E., 2000. Classification and regression trees: a powerful yet simple technique for ecological data analysis. Ecology 81, 3178–3192.

Everitt, B.S., Landau, S., Leese, M., 2001. Cluster Analysis, fourth ed. Arnold, 248 pp.

Field, C.B., 1991. Ecological scaling of carbon gain to stress and resource gain. In: Mooney, A., Winner, W.E. (Eds.), Response of Plants to Multiple Stresses. Academic Press, San Diego, CA, pp. 35–65.

Flanagan, L.B., Wever, L.A., Carlson, P.J., 2002. Seasonal and interannual variation in carbon dioxide exchange and carbon balance in a northern temperate grassland. Global Change Biol. 8, 599–615.

Gifford, R.M., 2003. Plant respiration in productivity models: conceptualisation, representation and issues for global terrestrial carbon-cycle research. Funct. Plant Biol. 30, 171–186.

Goetz, S.J., Prince, S.D., 1999. Modelling terrestrial carbon exchange and storage: evidence and implications of functional convergence in light-use efficiency. Adv. Ecol. Res. 28, 57–92.

Gower, S.T., Kucharik, C.J., Norman, J.M., 1999. Direct and indirect estimation of leaf area index, f_{APAR}, and net primary production of terrestrial ecosystems. Remote Sens. Environ. 70, 29–51.

Green, D.S., Erickson, J.E., Kruger, E.L., 2003. Foliar morphology and canopy nitrogen as predictors of light-use efficiency in terrestrial vegetation. Agric. For. Meteorol. 115, 163–171.

Gu, L., Baldocchi, D., Verma, S.B., Black, T.A., Vesala, T., Falge, E.M., Dowty, P.R., 2002. Advantages of diffuse radiation for terrestrial ecosystem productivity. J. Geophys. Res. 107 (D6), 40–50.

Hollander, M., Wolfe, D.A., 1999. Nonparametric Statistical Methods, second ed. Wiley–Interscience, New York, NY, 787 pp.

Ito, A., Oikawa, T., 2004. Global mapping of terrestrial primary productivity and light-use efficiency with a process-based model. In: Shiyomi, M., et al. (Eds.), Global Environmental Change in the Ocean and on Land. TERRAPUB, Tokyo, pp. 343–358.

Jarvis, P.G., Leverenz, J.W., 1983. Productivity of temperate deciduous and evergreen forests. In: Lange, O.L., Nobel, P.S., Osmond, C.B., Ziegler, H. (Eds.), Encyclopedia of Plant Physiology, Part IV, vol. 12D. Springer Verlag, Berlin, pp. 234–280.

Krzanowski, W.J., Lai, Y.T., 1988. A criterion for determining the number of groups in a data set using sum-of-squares clustering. Biometrics 44, 23–34.

Lagergren, F., Eklundh, L., Grelle, A., Lundblad, M., Mölder, M., Lankreijer, H., Lindroth, A., 2005. Net primary production and light use efficiency in a mixed coniferous forest in Sweden. Plant Cell Environ. 28 (3), 412–423.

Larcher, W., 1995. Physiological Plant Ecology. Springer Verlag, Berlin, 506 pp.

Lobell, D.B., Ortiz-Monasterio, I.J., Asner, G.P., Naylor, R.L., Falcon, W.P., 2005. Combining field surveys, remote sensing, and regression trees to understand yield variations in an irrigated wheat landscape. Agronomy J. 97, 241–249.

Mahrt, L., Vickers, D., 2002. Relationship of area-averaged carbon dioxide and water vapour fluxes to atmospheric variables. Agric. For. Meteorol. 112 (3–4), 195–202.

Mäkelä, A., Valentine, H.T., 2001. The ratio of NPP to GPP: evidence of change over the course of stand development. Tree Physiol. 21, 1015–1030.

McMurtrie, R.E., Gholz, H.L., Linder, S., Gower, S.T., 1994. Climatic factors controlling the productivity of pine stands: a model-based analysis. Ecol. Bull. 43, 173–188.

Medlyn, B.E., 1996. Interactive effects of atmospheric carbon dioxide and leaf nitrogen concentration on canopy light use efficiency: a modeling analysis. Tree Physiol. 16, 201–209.

Meek, D.W., Hatfield, J.L., Howell, T.A., Idso, S.B., Reginato, R.J., 1984. A generalized relationship between photosynthetically active radiation and solar radiation. Agronomy J. 76, 939–945.

Monteith, J.L., 1972. Solar radiation and production in tropical ecosystems. J. Appl. Ecol. 9, 747–766.

Monteith, J.L., 1977. Climate and the efficiency of crop production in Britain. Philos. Trans. R. Soc. Lond. B 281, 277–294.

Moore, T.R., Bubier, J.L., Lafleur, P.M., Frolking, S.E., Roulet, N.T., 2002. Plant biomass and production and CO_2 exchange in an ombrotrophic bog. J. Ecol. 90, 25–36.

Nichol, C.J., Huemmrich, K.F., Black, T.A., Jarvis, P.G., Walthall, C.L., Grace, J., Hall, F.G., 2000. Remote sensing of photosynthetic-light-use efficiency of boreal forest. Agric. For. Meteorol. 101 (2–3), 131–142.

Nichol, C.J., Lloyd, J., Shibistova, O., Arneth, A., Roser, C., Knohl, A., Matsubara, S., Grace, J., 2002. Remote sensing of photosynthetic light use efficiency of Siberian boreal forest. Tellus B 54 (5), 677–687.

Norby, R.J., Sholtis, J.D., Gunderson, C.A., Jawdy, S.S., 2003. Leaf dynamics of a deciduous forest canopy: no response to elevated CO_2. Oecologia 136 (4), 574–584.

Nouvellon, Y., LoSeen, D., Rambal, S., Begue, A., Moran, M.S., Kerr, Y., Qi, J., 2000. Time course of radiation use efficiency in a shortgrass ecosystem: consequences for remotely-sensed estimation of primary production. Remote Sens. Environ. 71, 43–55.

Potter, C.S., Klooster, S., Brooks, V., 1999. Interannual variability in terrestrial net primary production: exploration of trends and controls on regional to global scales. Ecosystems 2, 36–48.

Ruimy, A., Jarvis, P.G., Baldocchi, D.D., Saugier, B., Valentini, R., 1995. CO_2 fluxes over plant canopies and solar radiation: a review. Adv. Ecol. Res. 26, 1–63.

Ruimy, A., Kergoat, L., Bondeau, A., Participants of the Potsdam NPP Model Intercomparison, 1999. Comparing global models of terrestrial net primary productivity (NPP): analysis of differences in light absorption and light-use efficiency. Global Change Biol. 5 (Suppl. 1), 56–64.

Ruimy, A., Saugier, B., Dedieu, G., 1994. Methodology for the estimation of terrestrial net primary production from remotely sensed data. J. Geophys. Res. 99, 5263–5283.

Running, S.W., Nemani, R., Heinsch, F.A., Zhao, M., Reeves, M.C., Hashimoto, H., 2004. A continuous satellite-derived measure of global terrestrial primary production. BioScience 54 (6), 547–560.

Runyon, J., Waring, R.H., Goward, S.N., Welles, J.M., 1994. Environmental limits on net primary production and light-use efficiency across the Oregon transect. Ecol. Appl. 4, 226–237.

Ryan, M.G., Lavigne, M.B., Gower, S.T., 1997. Annual carbon cost of autotrophic respiration in boreal forest ecosystems in relation to species and climate. J. Geophys. Res. 102, 28871–28883.

Still, C.J., Randerson, J.T., Fung, I.Y., 2004. Large-scale plant light-use efficiency inferred from the seasonal cycle of atmospheric CO_2. Global Change Biol. 10, 1240–1252.

Turner, D.P., Ritts, W.D., Cohen, W.B., Gower, S.T., Zhao, M., Running, S.W., Wofsy, S.C., Urbanski, S., Dunn, A., Munger, J.W., 2003a. Scaling gross primary production (GPP) over boreal and deciduous forest landscapes in support of MODIS GPP product validation. Remote Sens. Environ. 88, 256–270.

Turner, D.P., Urbanski, S., Bremer, D., Wofsy, S.C., Meyers, T., Gower, S.T., Gregory, M., 2003b. A cross-biome comparison of daily light use efficiency for gross primary production. Global Change Biol. 9, 383–395.

Turner, D.P., Ritts, W.D., Cohen, W.B., Maeirsperger, T.K., Gower, S.T., Kirschbaum, A.A., Running, S.W., Zhai, M., Wofsy, S.C., Dunn, A.L., Law, B.E., Campbell, J.L., Oechel, W.C., Kwon, H.J., Meyers, T.P., Small, E.E., Kurc, S.A., Gamon, J.A., 2005. Site-level evaluation of satellite-based global terrestrial gross primary production and net primary production monitoring. Global Change Biol. 11, 666–684.

Whitehead, D., Beadle, C.L., 2004. Physiological regulation of productivity and water use in Eucalyptus: a review. For. Ecol. Manage. 193 (1–2), 113–140.

Whitehead, D., Gower, S.T., 2001. Photosynthesis and light-use efficiency by plants in a Canadian boreal forest ecosystem. Tree Physiol. 21, 925–929.

Witten, I.H., Frank, E., 2005. Data Mining: Practical Machine Learning Tools and Techniques, second ed. Morgan Kaufmann, San Francisco, CA, 525 pp.

Veroustraete, F., Sabbe, H., Rasse, D.P., Bertels, L., 2004. Carbon mass fluxes of forests in Belgium determined with low resolution optical sensors. Int. J. Remote Sens. 25 (4), 769–792.

Yeo, I.K., Johnson, R.A., 2000. A new family of power transformations to improve normality or symmetry. Biometrika 87, 954–959.